Journal of Thermal Analysis and Calorimetry, Vol. 88 (2007) 1, 251–260

INFLUENCE OF BARIUM SOURCE ON THE CHARACTERISTICS OF SOL-PRECIPITATED $BaTiO_3$ POWDERS AND RELATED CERAMICS

Adelina Ianculescu[1*], *Ana Brăileanu*[2], *M. Crişan*[2], *P. Budrugeac*[3], *N. Drăgan*[2], *G. Voicu*[1], *D. Crişan*[2] *and V. E. Marinescu*[3]

[1]Department of Oxide Materials Science and Engineering, 'Politehnica' University of Bucharest, 1–7 Gh. Polizu P.O. Box 12-134, 011061 Bucharest-1, Romania
[2]Institute of Physical Chemistry 'Ilie Murgulescu' of the Romanian Academy, 202 Splaiul Independenţei 060021 Bucharest-6, Romania
[3]INCDIE ICPE-CA, 313 Splaiul Unirii, 030138 Bucharest-3, Romania

In order to obtain pure and fine $BaTiO_3$ powders with controlled morphology, sol-precipitation methods involving the use of titanium iso-propoxide and of two different barium sources, i.e. barium nitrate and barium acetate, were proposed in this work. The thermal behaviour of the synthesized gels and the X-ray diffraction data obtained for the oxide powders pointed out that, by using $Ba(NO_3)_2$ as barium source, the decomposition process was completed at lower temperature (750°C) and was accompanied by a more pronounced tendency to obtain a single phase $BaTiO_3$ composition, by comparison with the synthesis where barium acetate was used as raw material (1100°C). Scanning electron microscopy investigations emphasized the effect of the nature of barium source and synthesis conditions on the morphology of the oxide powders, as well as on the microstructure of the related ceramics.

Keywords: *barium titanate, perovskite, sol-precipitation, thermal analysis, X-ray diffraction*

Introduction

The perovskite ceramics derived from $BaTiO_3$ (BT) were intensively investigated due to their unique properties (high permittivity, ferroelectricity and piezoelectricity), which makes them promising candidates for electronic applications such as multilayer ceramic capacitors (MLCC) [1], semiconductors with positive temperature coefficient of resistance (PTCR) [2, 3] and pyroelectric detectors. The mentioned characteristics strongly depend on raw materials and processing methods and conditions, so that efforts on the $BaTiO_3$ synthesis are still in progress, in order to obtain suitable microstructures and thus, to improve its electrical behaviour.

To obtain a fine, homogeneous and pore-less microstructure, it is necessary to start with preparing fine, stoichiometric and narrow size distribution powders, required in the last years as a result of the miniaturization trend in electrical applications. For this purpose, several wet chemical synthesis methods, involving the homogeneity of precursors at molecular level, as coprecipitation via oxalate route [4–6], polymeric precursors method (PPM) [7–9], hydrothermal [10–12] and sol-gel techniques [13–16], were proposed as alternative approach to the dry mixed-oxides processing, which presents the inconvenience of uncontrolled microstructures of the resulted ceramics and high sintering temperatures induced by the solid state reactions.

The sol-gel processing seems to be one of the most adequate methods to prepare nanoscaled $BaTiO_3$ particles. Although the simple alkoxides were mostly used as starting materials in the sol-gel technique [17, 18], because of their sensitivity to hydrolysis, an undesirable competition between hydrolysis and condensation may occur. In order to avoid this disadvantage, in the case of bimetallic oxides, the so-called 'semi-alkoxide' route, which consists in using as starting materials the acetate or nitrate of one metal and an alkoxide of another one, was proposed [19].

The aim of this work is to study the influence of both barium source and processing conditions on the structure and morphology of $BaTiO_3$ powders and on the microstructure of the related ceramics.

Experimental

Samples preparation

Four $BaTiO_3$ powders were prepared by sol-precipitation method using two different barium sources, i.e. barium nitrate (Merck) and barium acetate (Merck). In both cases $Ti(i\text{-}OC_3H_7)_4$ (Merck) was used as tita-

* Author for correspondence: a.ianculescu@rdslink.ro

1388–6150/$20.00

Akadémiai Kiadó, Budapest, Hungary
Springer, Dordrecht, The Netherlands

nium source. First, we tried to reproduce a sol-gel procedure using the barium acetate as raw material, reported earlier by Mazdiyasni *et al*. [20]. Since even after high temperature processing, only a multiphase powder and very porous ceramics were obtained, we modified some of the synthesis conditions. The details concerning the molar ratio of the precursors and the reaction conditions of the different syntheses performed in this work are summarized in Table 1. In all cases, Ti-alkoxide and Ba-salt precursors in equistoichiometric quantities ($BaO:TiO_2$ =1:1) were used. One can notice that the difference between syntheses 1 and 2 consists only in the presence of the HNO_3 as catalyst (indicated by the dashed lines in the flowchart of Fig. 1) in the last one. Regarding the sol-precipitation procedures where barium nitrate was used as raw material, it have to be mentioned that unlike synthesis 3, in synthesis 4 $Ba(NO_3)_2$ was first solved in boiled water.

The obtained precursors were thermally treated in air, up to 850°C (precursors 1, 3 and 4) and 1100°C (precursor 2), with a 2 h plateau at the mentioned temperatures. A heating rate of 1°C min^{-1} was used for the complete removal of the residual carbon resulted from the decomposition of the organic matter. The flowcharts of precursors and oxide powders preparation by the proposed sol-precipitation procedures are presented in Figs 1 and 2.

The calcined powders were uniaxially pressed into pellets of 13 mm diameter and ~3 mm thickness, which were then sintered for 4 h in air, at 1300°C. Some intermediate thermal treatments were performed at 550 and 750°C, respectively, in order to estimate the mechanism of the perovskite phase formation.

Intrumental methods

In order to determine the changes which occur during the heating process, thermal analysis measurements

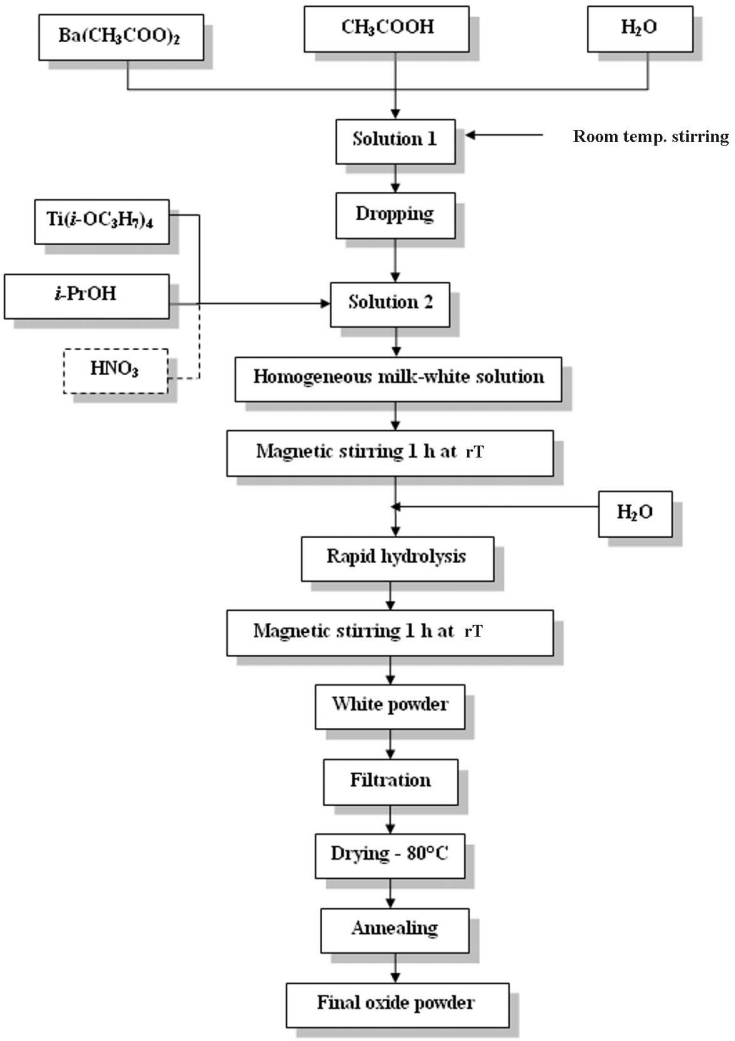

Fig. 1 Flowchart for the sol-precipitation syntheses 1 and 2

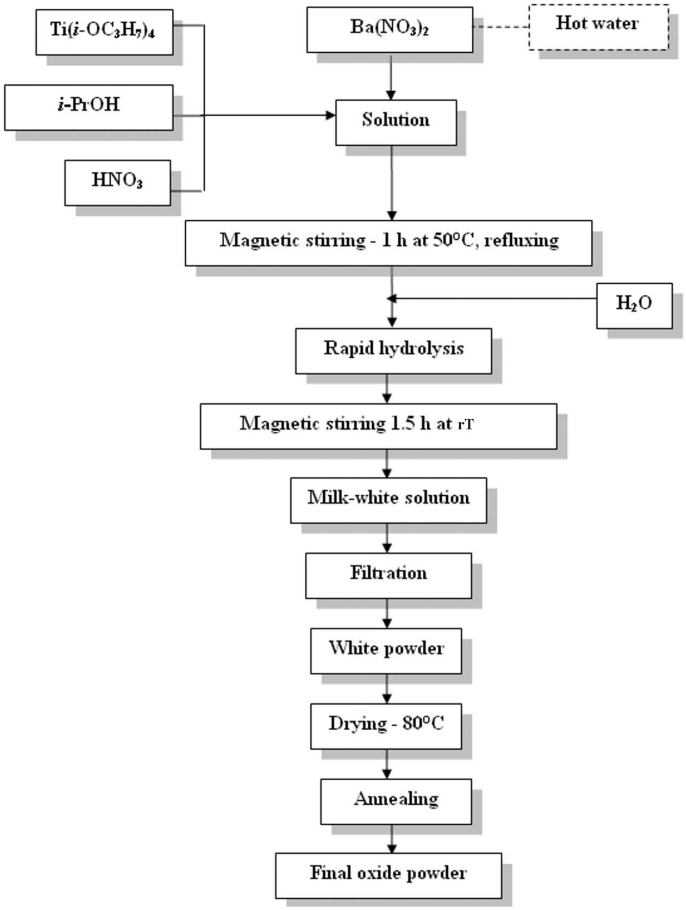

Fig. 2 Flowchart for the sol-precipitation syntheses 3 and 4

of the precursors were performed up to 1000°C in static air atmosphere, with a heating rate of 10 K min^{-1} using Pt crucibles, with a Derivatograph, supplied by MOM Hungary, system Paulik–Paulik–Erdey, type Q1500D. In addition, DSC and TG/DTG investigations were performed up to 1200°C in static air atmosphere, with the same heating rate, using a STA 409 PC Luxx simultaneous DSC and TG/DTG equipment (NETZSCH, Germany).

Room temperature X-ray diffraction measurements used to investigate the purity of the perovskite phase, were performed with a SHIMADZU XRD 6000 diffractometer, using Ni-filtered CuK_α radiation (λ=1.5418 Å), with a scan step of 0.02° and a counting time of 1 s/step, for diffraction angles 2θ ranged between 20 and 80°. To estimate the structural characteristics (lattice parameters, crystallite sizes and internal microstrains) a counting time of 10 s/step, for 2θ ranged between 20°/120° was used. The lattice constants calculation is based on the least squares procedure (LSP), using the linear multiple regressions for several XRD lines, depending on the unit cell symmetry. The average values of both the crystallite size and the internal microstrains were determined from at least 10 diffractions lines indexed from the major tetragonal phase.

A HITACHI S2600N scanning electron microscope coupled with EDX was used to analyse the morphology and agglomeration tendency of the synthesized powders, as well as the microstructure of the resulted ceramics and to check the stoichiometry of the samples.

Results and discussions

Thermal behaviour

All gel powders investigated show a relatively small (up to ~7%) initial mass loss at ~60–80°C resulting from the evaporation of alcohol and desorption of the adsorbed moisture. This effect is more visible for the powders derived from barium acetate.

Figure 3 shows the thermal behaviour of the powdered precursor prepared by synthesis no. 1. The exothermic effects at 318 and 344°C on DTA curve are due to the combustion of the organic matter of the precursor. The mass loss recorded on the TG curve seems to be constant between 550 and 950°C.

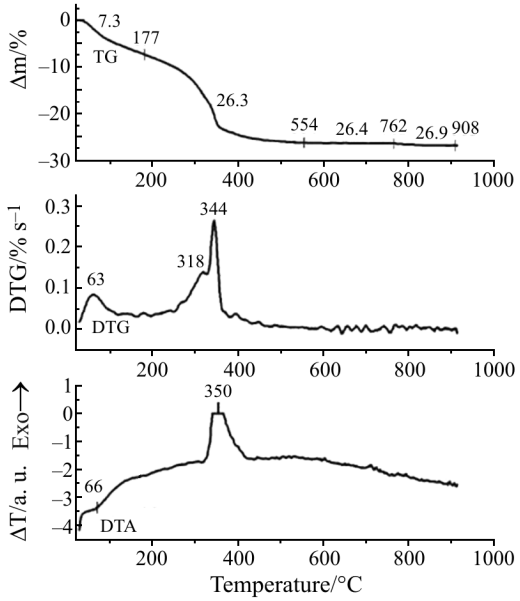

Fig. 3 Thermal behaviour of the precursor prepared according to the procedure no. 1. BaTi – precursor 1 (barium acetate source), β=10 K min^{-1}, *m*=39.1 mg, static air

Probably, the solid state reactions, involving the perovskite formation take place at higher temperatures in these non-isothermal conditions. This is why synthesis no. 2, which is very alike with the synthesis no. 1, was performed. The precursor obtained in this case was also investigated by thermal analysis methods, but this time the heating was carried out up to 1200°C (Fig. 4). TG/DTG and DSC curves show that all the interaction processes are ended at ~1100°C, because no mass loss on TG curve and no effect on DSC curve are recorded above this temperature.

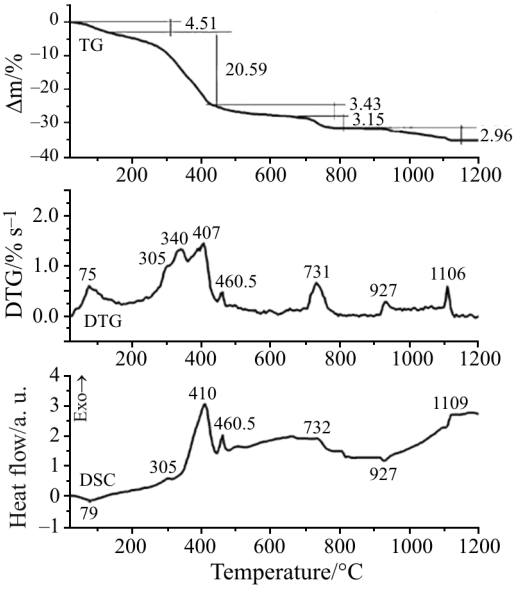

Fig. 4 Thermal behaviour of the precursor prepared according to the procedure no. 2. BaTi – precursor 2 (barium acetate source), β=10 K min^{-1}, *m*=16.2 mg, static air

In case of gel precursors derived from barium acetate, probably the exothermic processes due to the combustion of the organic compounds and crystallization of barium titanates strongly overlap the endothermic decomposition reactions. For the gel precursors derived from barium nitrate (Figs 5 and 6, respectively), the decomposition processes are well marked on DTA curves (much more pronounced for the precursor 4) and they are practically ended at ~ 700°C.

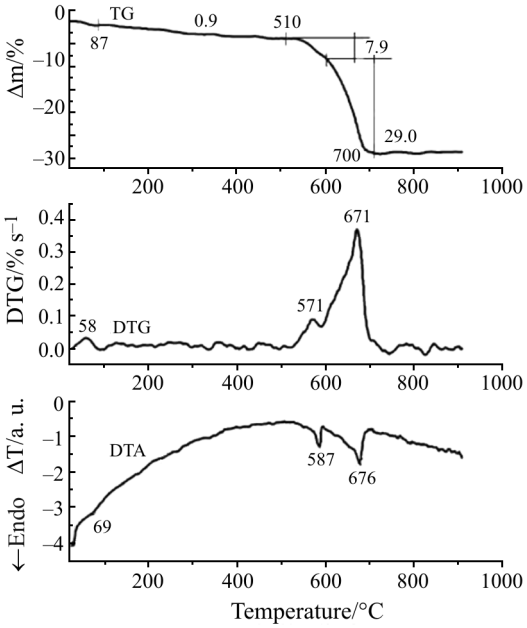

Fig. 5 Thermal behaviour of the precursor prepared according to the procedure no. 3. BaTi – precursor 3 (barium nitrate source), β=10 K min^{-1}, *m*=42.5 mg, static air

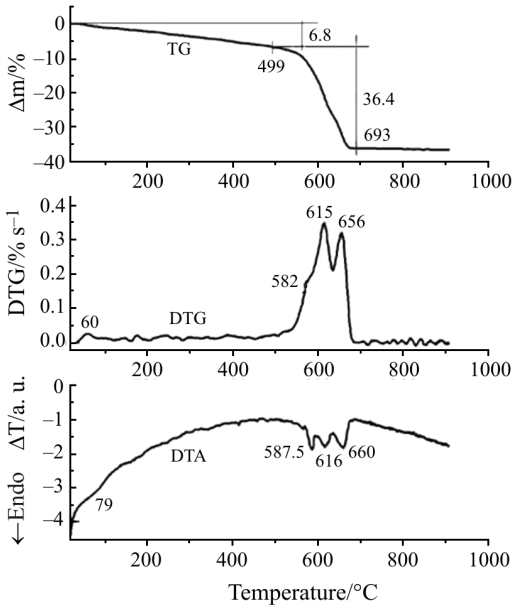

Fig. 6 Thermal behaviour of the precursor prepared according to the procedure no. 4. BaTi – precursor 4 (barium nitrate source), β=10 K min^{-1}, *m*=42.8 mg, static air

Phase composition

It is well known that the sol-gel technique is very sensitive to the raw materials used [21]. For the oxide powders obtained after annealing at 850°C from precursors derived from barium acetate the X-ray investigations revealed that, beside the major perovskite $BaTiO_3$ phase (JCPDS no. 79-2265), barium carbonate (witherite), with an orthorhombic structure (JCPDS no. 5-378) and also barium- or titanium-rich oxide compounds as Ba_2TiO_4 (JCPDS no. 38-1481) or/and $BaTi_2O_5$ (JCPDS no. 70-1188) were identified as secondary phases (Fig. 7), irrespective of the presence or lack of the catalyst. These results are in good agreement with these ones reported by Beck *et al.* [21] for their sol-gel powders obtained via acetate route, showing that at 850°C (for 2 h plateau) the chemical reactions are not completed. The witherite is the intermediate compound resulting from the decomposition of the gel precursor at lower temperatures, as one can notice from the X-ray diffraction pattern recorded at room temperature for the powder synthesized by procedure no. 1 and annealed at 550°C (Fig. 7). The high background of the diffractogram indicates the presence of a large amount of a quasi-amorphous phase, most probably consisting of nanoscaled titanium-rich particles, which at higher temperatures will react with $BaCO_3$ to form the perovskite skeleton of the barium titanate, according to the reaction (1):

$$BaCO_3+TiO_2 \rightarrow BaTiO_3+CO_2\uparrow \quad (1)$$

Therefore, for the sol-precipitation acetate route higher temperatures are required in order to obtain single-phase perovskite powders. The X-ray diffraction pattern for the oxide powder synthesized by procedure no. 2 pointed out an almost pure barium titanate phase after annealing at 1100°C, for 2 h (Fig. 8). In the temperature range of 850–1100°C the following solid state reactions could take place:

$$BaCO_3+BaTi_2O_5 \rightarrow 2BaTiO_3+CO_2\uparrow \quad (2)$$

$$Ba_2TiO_4+BaTi_2O_5 \rightarrow 3BaTiO_3 \quad (3)$$

X-ray diffraction patterns of the powders derived from barium nitrate (synthesis no. 3 and 4), presented in Figs 9 and 10, show a well crystallized $BaTiO_3$ phase. After annealing at 850°C, only small amount of barium

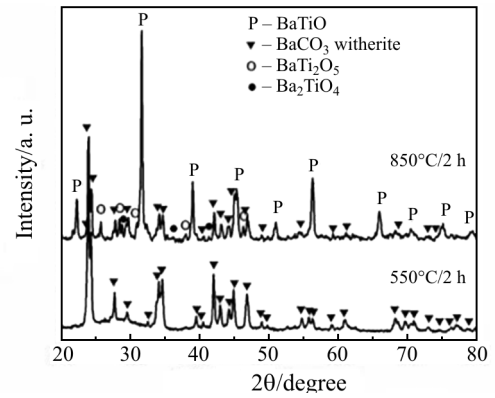

Fig. 7 Room temperature X-ray diffraction pattern for powder no. 1, annealed for 2 h at 550 and 850°C, respectively

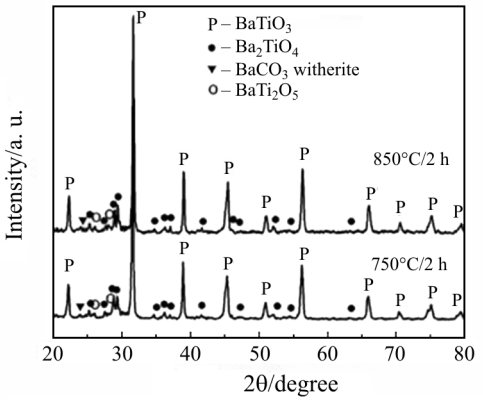

Fig. 9 Room temperature X-ray diffraction pattern for powder no. 3, annealed for 2 h at 750 and 850°C, respectively

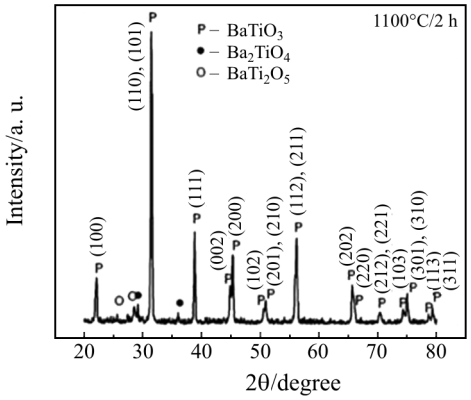

Fig. 8 Room temperature X-ray diffraction pattern for powder no. 2, annealed at 1100°C for 2 h

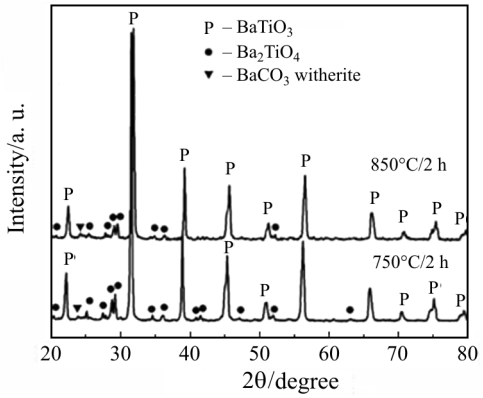

Fig. 10 Room temperature X-ray diffraction pattern for powder no. 4, annealed for 2 h at 750 and 850°C, respectively

Table 1 Processing parameters of the sol-gel syntheses

Sample	Metallic precursors	Molar ratio				pH mixture	Reaction conditions	
		$\frac{CH_3COOH}{\sum metallic\ precursors}$	$\frac{i\text{-}C_3H_7OH}{\sum metallic\ precursors}$	$\frac{H_2O}{\sum metallic\ precursors}$	$\frac{HNO_3}{\sum metallic\ precursors}$		T/°C	t/h
[20]	$Ba(CH_3COO)_2$+ $Ti(i\text{-}O_3H_7)_4$	1.19	–	20.69	0.298	3–4	50	2
1.	$Ba(CH_3COO)_2$+ $Ti(i\text{-}O_3H_7)_4$	0.44	2	45.83	–	4–5	20	2
2.	$Ba(CH_3COO)_2$+ $Ti(i\text{-}O_3H_7)_4$	0.44	2	45.83	0.152	3–4	20	2
3.	$Ba(NO_3)_2$+ $Ti(i\text{-}O_3H_7)_4$	–	5.92	25	0.271	3–4	50	2
4.	$Ba(NO_3)_2$+ $Ti(i\text{-}O_3H_7)_4$	–	5.92	27.78	0.217	3–4	50	2

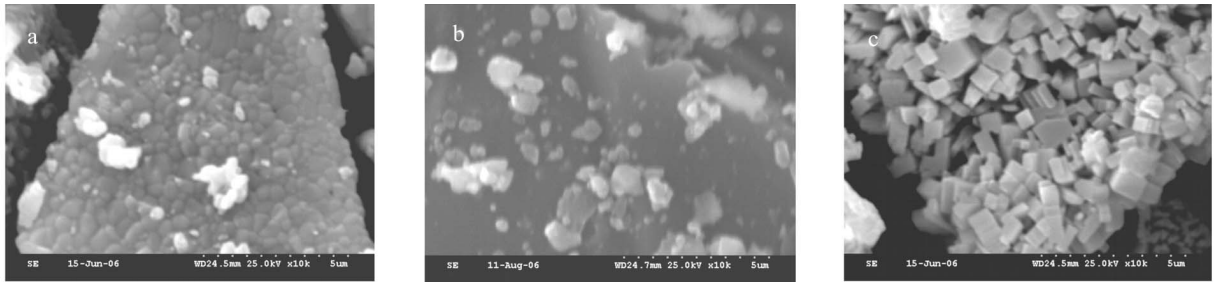

Fig. 11 SEM images of powders synthesized by: a – procedure no. 2 and annealed at 1100°C/2 h; b – procedure no. 3 and annealed at 850°C/2 h and c – procedure no. 4 and annealed at 850°C/2 h

orthotitanate (Ba_2TiO_4) and barium polytitanate ($BaTi_2O_5$), probably obtained because of the slow heating rate of 1°C min^{-1}, were identified as non-equilibrium phases at the detection limit. Therefore, we concluded that the nitrate procedure leads to a single phase composition at lower annealing temperatures, by comparison with the acetate route. These results are in agreement with the thermal analysis data.

Structural parameters

It is well known from the literature data that, below a critical crystallite size, which for the sol-gel method was estimated at ~50 nm [22–24], the symmetry of the $BaTiO_3$ unit cell becomes difficult to be assigned, because of the structural distortions and internal strains which occur in such nanostructured systems. Moreover, below 30 nm it seems that only the cubic structure is present, which means that the $BaTiO_3$ ferroelectricity is cancelled. In our case, the structural parameters are summarized in Table 2. Some interesting aspects must be pointed out:

i) powders obtained by acetate route and annealed at lower temperatures (750–850°C) consist of a mixture of two $BaTiO_3$ forms with different symmetries, a tetragonal and a cubic one. Since the major phase exhibits a tetragonal structure, the lattice parameters were calculated only for this form. The powder particles become entirely tetragonal at higher annealing temperature (above 1000°C). The rise of the calcination temperature induces the growth of the crystallites and, consequently, the decrease of the internal microstrains, specific mainly to the nanostructured materials. The crystallite size strongly influences the tetragonality degree, expressed as *c*/*a* ratio. Larger crystallites imply a more relaxed structure so that, the tetragonality degree increases.

ii) powders synthesized by nitrate route are 'unusual' from the structural point of view. A particular tetragonal $BaTiO_3$ phase characterized by a subunitary *c*/*a* ratio was determined for these powders (excepting sample 4 at 750°C). This distorted phase, known in the literature as the 'in plane' tetragonal phase, was predicted by Pertsev *et al*. [25] for the strained epitaxial $BaTiO_3$ thin films and it was also reported by Wada *et al.* [26] for their nanopowders obtained by a modified two-step oxalate decomposition route. Very small amounts of cubic form were detected only in the sample 3, calcined at 750°C. Taking into account also the errors, it seems that, for powders derived from barium nitrate, the annealing temperature do not influences considerably the average crystallite size, unlike the samples derived from barium acetate.

Powders morphology

The powders morphology was analysed only for the samples tending to a single phase composition. The powder synthesized by acetate route and annealed at 1100°C for 2 h consists of large conglomerates of polycrystalline particles with an average size of ~500 nm (Fig. 11a). The samples obtained from barium nitrate consist of particles, which exhibit different morphology, depending on the preparation procedure. Thus, whereas in SEM image for sample no. 3 (Fig. 11b), spherical particles with pronounced tendency to form agglomerates were noticed, the powder no. 4 consists of cubic and tetragonal-shaped isolated and almost microscaled particles (Fig. 11c), which seems to be rather polycrystalline, taking into account the crystallite average size determined by XRD. However, in order to determine exactly the size of the powders particles and their single- or polycrystalline nature, further transmission electron microscopy (TEM) coupled with selected area electron diffraction (SAED) investigations are required.

Ceramics microstructure

Ceramics elaborated from the synthesized powders exhibit relative density values of ~87–94%. For the ceramic samples obtained from powders prepared via acetate route, the catalyst and the annealing temperature of the powder do not influence the microstructural features. The SEM image of the sample derived from powder no. 2, sintered at 1300°C, for 4 h (Fig. 12a), shows a dense, fine, pore-less, bimodal microstructure, consist-

Table 2 Structural parameters of the synthesized $BaTiO_3$ powders

Sample	Annealing temperature/°C	Precursor	$BaTiO_3$ form	Structural parameters				Crystallite size, $\langle D \rangle$/Å	Internal microstrain, $\langle S \rangle \times 10^3$
				Lattice constants		Tetragonality, c/a	Unit cell volume, V/Å^3		
				a/Å	c/Å				
1.	850	barium acetate	T*+C**	4.0064(64)	4.0344(181)	1.0070(61)	64.76(50)	613(32)	0.34(5)
2.	750	barium	T+C	3.9994(33)	4.0182(92)	1.0047(31)	64.27(25)	429(34)	0.50(11)
	850	acetate	T+C	3.9960(39)	4.0221(108)	1.0065(37)	64.23(30)	616(35)	0.19(5)
	1100		T	4.0006(11)	4.0340(31)	1.0083(11)	64.56(8)	970(13)	0.15(2)
3.	750	barium	T+C	4.0027(17)	3.9820(48)	0.9948(16)	63.80(13)	509(20)	0.22(5)
	850	nitrate	T	3.9961(14)	3.9818(38)	0.9964(13)	63.58(10)	548(50)	0.21(10)
4.	750	barium	T	3.9973(14)	4.0128(39)	1.0039(13)	64.12(11)	500(16)	0.37(4)
	850	nitrate	T	3.9877(26)	3.9653(70)	0.9944(24)	63.06(19)	484(53)	0.30(16)

*T – tetragonal; **C – cubic

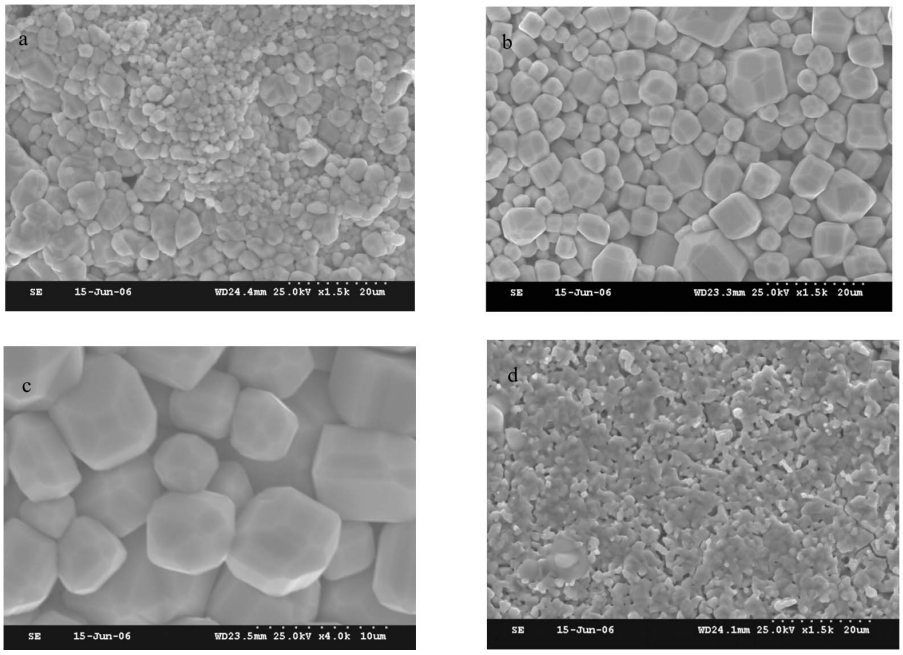

Fig 12 SEM images of the related ceramics sintered in air at 1300°C/4 h and elaborated from: a – powder no. 2; b – powder no. 3 – general view; c – powder no. 3 – detail and d – powder no. 4

ing of smaller (~1.5 μm), spherical or ovoid-shaped grains and larger grains (of ~10 μm).

In case of samples elaborated from powders prepared via nitrate route and sintered in the same conditions, the synthesis procedure strongly influences the ceramics microstructure. Thus, while the procedure 3 leads to a homogeneous and still bimodal microstructure, in which the smaller grains (of ~2.5 μm) coexist with larger grains (~15 μm), exhibiting a polyhedral form with extremely well defined faces and edges (Figs 12b, c), by the procedure no. 4, an unexpected fine-grained microstructure with some intergranular pores and smaller grains (~1.5 μm) with undefined boundaries and junctions was obtained (Fig. 12d).

Conclusions

The thermal behaviour of the synthesized gel precursors and the X-ray diffraction data obtained for the oxide powders pointed out that, by using $Ba(NO_3)_2$ as barium source, the decomposition process was completed at lower temperature (750°C) and was accompanied by a more pronounced tendency to obtain a single phase $BaTiO_3$ composition, by comparison with the synthesis where barium acetate was used as raw material. In the last case temperatures above 1100°C are required to obtain pure barium titanate.

From structural point of view, the powders prepared via acetate procedure and calcined at lower temperatures (750–850°C) consist of a mixture of tetragonal and cubic $BaTiO_3$ forms and become entirely tetragonal after annealing at temperatures above 1000°C. The powders derived from barium nitrate exhibit mainly a particular tetragonal structure with a subunitary *c*/*a* ratio, specific only to the strongly distorted nanostructured $BaTiO_3$ systems.

The influence of annealing temperature on the $BaTiO_3$ structural characteristics is more obvious for the powders synthesized via acetate procedure, where the rise of temperature induces a faster increase of the tetragonality degree and crystallite average size, and, consequently, a decrease of the internal microstrains.

The morphology of the oxide powders is related to the barium source, synthesis conditions and annealing temperature. For the powders derived from the same barium source, i.e. barium nitrate, even small changes in the synthesis procedure can induce significant modifications of the shape and size of particles and of their agglomeration tendency.

The same factors obviously influence also the relative density and the microstructural features (grain size and shape and porosity) of the related ceramics. The most dense and uniform microstructure, consisting of very well faceted grains, was obtained from samples elaborated from powders prepared via sol-precipitation nitrate procedure no. 3.

Acknowledgements

This work was supported by two Romanian grants (CNCSIS type A and CEEX).

References

1 S. Schlag and H. F. Eicke, Solid State Commun., 91 (1994) 883.
2 H. A. Sauer and J. R. Fisher, J. Am. Ceram. Soc., 43 (1960) 297.
3 W. Heywang, J. Mater. Sci., 6 (1971) 1214.
4 S. Otta and S. D. Bhattamisra, J. Therm. Anal. Cal., 41 (1994) 419.
5 M. Stockenhuber, H. Mayer and J. A. Lercher, J. Am. Ceram. Soc., 76 (1995) 1185.
6 H. S. Potdar, S. B. Deshpande and S. K. Date, Mater. Chem. Phys., 58 (1999) 121.
7 W. -S. Cho, J. Phys. Chem. Solids, 59 (1998) 659.
8 P. Durán, F. Capel, J. Tartaj and C. Moure, J. Mater. Res., 16 (2001) 197.
9 J. -D. Tsay, T. -T. Fang, T. A. Gubiotti and J. Y. Ying, J. Mater. Sci., 33 (1998) 3721.
10 J. O. Eckert Jr., C. C. Hung-Houston, B. L. Gersten, M. M. Lencka and R. E. Riman, J. Am. Ceram. Soc., 79 (1996) 2929.
11 R. Vivekanandan and T. R. N. Kutty, Powder Technol., 57 (1989) 181.
12 S. W. Lu, B. I. Lee, Z. L. Wang and W. D. Samuels, J. Cryst. Growth, 219 (2000) 269.
13 P. P. Phule and S. H. Risbud, Adv. Ceram. Mater., 3 (1988) 183.
14 G. Pfaff, J. Mater. Chem., 2 (1992) 591.
15 Ch. Lemoine, B. Gilbert, B. Michaux, J. -P. Pirard and A. J. Lecloux, J. Non-Cryst. Solids, 175 (1994) 1.
16 C. Zhixiong, Z. Fangaqiao, L. Meidong, W. Guoan and P. Xiangsheng, Ferroelectrics, 123 (1991) 61.
17 D. P. Birnie III, M. H. Jilavi, T. Krajevski and R. Nab, J. Sol-Gel Sci. Technol., 13 (1998) 855.
18 T. Yogo, K.-I. Kikuta, S. Yamada and S.-I. Hirano, J. Sol-Gel Sci. Technol., 2 (1994) 175.
19 O. G. Dediu, M. Crişan, Gh. Aldica and M. Zaharescu, Rev. Roum. Chim., 49 (2004) 811.
20 K. S. Mazdiyasni, R. T. Dolloff and J. S. Smith, J. Am. Ceram. Soc., 52 (1969) 523.
21 H. P. Beck, W. Eiser and R. Haberkorn, J. Eur. Ceram. Soc., 21 (2001) 687
22 J. M. Wilson, Am. Ceram. Soc. Bull., 74 (1995) 106.
23 X. Li and W. Shih, J. Am. Ceram. Soc., 80 (1997) 2844.
24 S. Aoyagi, Y. Kuroiwa, A. Sawada, H. Kawaji and T. Atake, J. Therm. Anal. Cal., 81 (2005) 627.
25 N. A. Pertsev, A. G. Zembilgotov and A. K. Tagantsev, Phys. Rev. Lett., 80 (1998) 1988.
26 M. Yashima, T. Hoshina, D. Ishimura, S. Kobayashi, W. Nakamura, T. Tsurumi and S. Wada, J. Appl. Phys. 98 (2005), 014313-1.

DOI: 10.1007/s10973-006-8083-3